Formulation of an Explicit-Multiple-Time-Step Time Integration Method for Use in a Global Primitive Equation Grid Model

WINSTON C. CHAO[1]

Science Applications, Inc., McLean, VA 22102

(Manuscript received 10 May 1981, in final form 13 July 1982)

ABSTRACT

With appropriate modifications, a recently proposed explicit-multiple-time-step scheme (EMTSS) is incorporated into the UCLA model. In this scheme, the linearized terms in the governing equations that generate the gravity waves are split into different vertical modes. Each mode is integrated with an optimal time step, and at periodic intervals these modes are recombined. The other terms are integrated with a time step dictated by the CFL condition for low-frequency waves. This large time step requires a special modification of the advective terms in the polar region to maintain stability. Test runs for 72 h show that EMTSS is a stable, efficient and accurate scheme.

1. Introduction

In an explicit time integration of primitive equations, the time step is limited by the Courant–Friedrichs–Lewy (CFL) condition (Courant *et al.*, 1928). This limit is inversely related to the fastest phase speed in the model, which is the speed of the external gravity wave. Therefore, the explicit integration is rather slow. Since meteorologically significant waves have speeds much slower than that of the external gravity wave and possess practically all of the energy of the atmospheric motion, the use of the explicit scheme is uneconomical. Two major approaches have been taken to circumvent this difficulty. In the first approach, the linearized terms of the primitive equations that govern the gravity waves are integrated implicitly, and the remaining terms are integrated explicitly, with a time step dictated by the CFL condition for slow moving waves. Known as the semi-implicit scheme (SIS), it has been used both in grid point models (Kwizak and Robert, 1971) and in spectral models (Robert, 1969), with significant savings in computing time and acceptable accuracy (Robert *et al.*, 1972). However, since the speed of the gravity waves is reduced in the implicit integration, its accuracy is questionable in the regions of gravity wave excitation (Messinger and Arakawa, 1976), where correct simulation of the geostrophic adjustment process depends upon the correct treatment of gravity waves.

The second approach to expedite the integration involves separating the terms related to the gravity waves from the rest of the equations. One group of terms is first integrated with an optimal time step, either explicitly or implicitly, and the result of this step is used at the beginning of the marching for the other group, employing a different optimal time step. This is called the splitting method (Marchuk, 1974; Gadd, 1978). When explicit schemes are used, the splitting method does not have the adverse effect of retarding the gravity waves. However, since the different dynamic processes are calculated one at a time, the truncation errors of all steps are multiplied rather than added.

In a study which combined these two approaches, Burridge (1975) further separated the linearized terms governing gravity waves into different vertical modes. In this scheme, modes with phase speeds greater than those of the meteorological waves (usually the external gravity wave and the first two or three internal gravity waves) are integrated implicitly. The other terms are integrated explicitly as a second group. This method is known as split semi-implicit scheme (SSIS).

In a recent work, Madala (1981) proposed an explicit-multiple-time-step scheme[2] (EMTSS), which combines many of the advantages of the previously mentioned methods. In EMTSS, linearized terms in the primitive equation governing gravity waves are decomposed into different vertical modes. Modes with phase speeds greater than the meteorological

[1] Present affiliation: Code 964, Laboratory for Planetary Atmospheres, NASA/Goddard Space Flight Center, Greenbelt, MD 20771.

[2] The name comes from a reviewer's suggestion. Madala used the name "split-explicit;" which was already used by other authors for a different scheme (e.g., Gadd, 1978).

0027-0644/82/111603-15$07.75

waves are integrated explicitly and separately, with time steps allowed by the respective CFL conditions, and are recombined at periodic intervals. The other modes and the remaining terms are then integrated explicitly with a time step determined by the speed of the slow moving waves, which is usually five times as large as the time step allowed for the fastest moving waves. The basic procedure of this scheme is given in the next section.

Thus far, the EMTSS has been successfully applied to a tropical cyclone model (Madala, 1981). The speed of integration was increased by a factor of three over that using the explicit method and was slightly higher than that of the SIS. The results also showed almost the same accuracy as SIS and SSIS. The present paper presents a further investigation of the EMTSS to ascertain whether it also works in a global model, in which more complexities exist, such as high terrain and the diminishing zonal grid size toward the poles. The model chosen for this effort is the 1977 version of the UCLA model (Arakawa and Lamb, 1977; hereafter referred to as AL).

2. The basic procedure of EMTSS

The basic procedure of EMTSS can easily be illustrated starting with a one dimensional shallow water model. The governing equations for such a model on an f-plane are

$$\frac{\partial u}{\partial t} + \frac{\partial \phi}{\partial x} = A_u ,$$

$$\frac{\partial \phi}{\partial t} + \Phi \frac{\partial u}{\partial x} = A_\phi ,$$

where u is the velocity, ϕ and Φ are the perturbed and mean geopotentials respectively. A_u and A_ϕ represent the nonlinear [including $(\Phi - \phi)\partial u/\partial x$] terms (in a full model, A's would include a Coriolis force term). Physics terms are not involved in EMTSS formulation. The linearized gravity wave terms ($\partial\phi/\partial x$ and $\Phi\partial u/\partial x$) and the A's will be treated differently in EMTSS. Let Δt_g be the CFL time step limit based on the speed of the gravity waves. That is, $\Delta t_g = \epsilon\Delta x/(g\Phi)^{1/2}$, where Δx is the horizontal grid size and ϵ is a constant depending on the time scheme used ($\epsilon = 1$ for leapfrog scheme). Also, let Δt be the CFL time step limit for the system when $\partial\phi/\partial x$ and $\Phi\partial u/\partial x$ terms are excluded. Normally, Δt is greater than Δt_g.

If the leapfrog scheme is used, let us assume that the values of u and ϕ are known at t_1 and t_2 ($t_2 = t_1 + \Delta t$). The way to obtain values at t_2 when t_1 is the initial time will be considered shortly. Let $\Delta\tau$ be an integral fraction of Δt, $\Delta\tau = \Delta t/n$, where n is the smallest integer such that $\Delta\tau < \Delta t_g$. Then, the first stage of EMTSS is to replace the A's by their values evaluated at t_2. The second stage is to march explicitly the replaced equations (i.e., with fixed A's) from t_1 to t_3 ($t_3 = t_1 + 2\Delta t$) using time step $\Delta\tau$. Here, the first step marching can be done with a Matsuno scheme, and the remaining steps with a leapfrog scheme. A byproduct of the second stage will be a new set of u and ϕ at t_2. They are not retained for later use. Once u and ϕ at t_3 are obtained, the two stages are repeated. A's at t_3 will be evaluated and will replace the A's in the equations. Then the explicit marching from t_2 to t_4 with time step $\Delta\tau$ starts.

To obtain values of u and ϕ at t_2 when t_1 is the initial time, a two-level scheme has to be invoked, for example, the Matsuno scheme. In the first part of the Matsuno scheme, the A's in the equations are replaced by their values evaluated at t_1. The equations are marched to t^*, a temporary t_2. The second part of the Matsuno scheme is to march the equations again from t_1 to t_2 but this time the A's are replaced by their values evaluated at t^*.

In EMTSS, the linearized gravity wave terms and the A's are integrated explicitly with time steps less than their respective CFL limits. Therefore, the linear stability of the scheme is obvious. The efficiency of the scheme derives from not having to evaluate A's, which includes complicated computation of the nonlinear terms, at every $\Delta\tau$ interval. The EMTSS treats A's the same way as the SIS does. The linearized gravity wave terms are treated explicitly with time step $\Delta\tau$, rather than implicitly with time step Δt as in the SIS. Thus, the accuracy of the EMTSS is expected to be better than that of the SIS.

When the above procedure is followed in a K level primitive equation model, the number of equations that have to be marched in the second stage is $3K + 1$, ($2K$ momentum equations, K temperature equations and a surface pressure equation). This number can be greatly reduced by adopting the modal decomposition method (Burridge, 1975), and marching different modes separately with different optimal $\Delta\tau$. Thus, the efficiency is further improved. Also the two stages can be cast in a slightly different, though equivalent, version. Details of these approaches will be presented in the next section.

3. Formulation of EMTSS for a primitive equation global grid model

a. *Basic equations*

The vertical coordinate in the UCLA model is

$$\sigma \equiv (p - p_T)/\pi, \tag{1}$$

where p is pressure, p_T is a constant pressure at the model top (currently $p_T = 50$ mb), $\pi \equiv p_s - p_T$, and p_s is the pressure at the surface. Because there is only one layer in the stratosphere, the original definition of σ in the stratosphere (AL, p. 207) is not used for reasons of simplicity. All notations follow those of

AL, unless otherwise indicated. The symbols $\langle\ \rangle$ and $[\ ]$ indicate column vector and matrix respectively.

The zonal momentum equation in the flux form is

$$\frac{\partial}{\partial t}(\pi u) + \frac{\partial}{\partial x}(\pi u^2) + \frac{1}{\cos^2\phi}\frac{\partial}{\partial y}(\pi uv\cos^2\phi) + \frac{\partial}{\partial \sigma} \times (\pi u\dot{\sigma}) - \pi f v = -\pi\left(\frac{\partial \phi}{\partial x}\right)_\sigma - (\pi\sigma\alpha)\left(\frac{\partial \pi}{\partial x}\right)_\sigma + \pi F_x, \tag{2}$$

where u is the zonal velocity, v the meridional velocity, α the specific volume, f the Coriolis parameter, ϕ the latitude and geopotential (the distinction is obvious), λ the longitude, a the earth's radius, F_x the zonal frictional force, $\dot{\sigma} = d\sigma/dt$, $\partial x = a\cos\phi\partial\lambda$, and $\partial y = a\partial\phi$.

Since $\phi = \phi_s + \phi_a$, where ϕ_s is the surface value of ϕ, and ϕ_a is $\phi - \phi_s$, the pressure gradient force term in (2) can be written as

$$-\frac{\partial}{\partial x}(\pi\phi_a) + \{\overline{\overline{(\phi_a - \sigma\pi\alpha)}} + (\phi_a - \sigma\pi\alpha)'\} \times \frac{\partial}{\partial x}\pi - \pi\frac{\partial}{\partial x}\phi_s,$$

where the double overbar denotes the time and global horizontal average on a σ-surface, and the prime denotes the deviation from it. If

$$\Phi \equiv \pi\phi_a - \overline{\overline{(\phi_a - \sigma\pi\alpha)}}\pi,$$

(2) becomes

$$\frac{\partial}{\partial t}(\pi u) + \frac{\partial}{\partial x}\bar{\bar{\Phi}} = R_u, \tag{3}$$

where R_u denotes all remaining terms, which vary slowly in time compared with the linear gravity wave terms. The additional smoothing operator, denoted by the dashed overbar, suppresses the amplitude of the short waves to overcome the problem associated with diminishing zonal grid size toward the poles. This operator is fully described in AL (p. 248) and is applied to the zonal pressure gradient term and to the zonal mass flux term. In a similar manner, the meridional momentum equation can be written as

$$\frac{\partial}{\partial t}(\pi v) + \frac{\partial}{\partial y}\Phi = R_v. \tag{4}$$

Next, the continuity equation can be integrated vertically to give

$$\frac{\partial}{\partial t}\pi + \langle \mathbf{N}_2\rangle^T\langle \mathbf{D}\rangle = 0, \tag{5}$$

where

$$D \equiv \nabla\cdot(\pi\mathbf{v}) = \frac{\partial}{\partial x}(\bar{\bar{\pi}}\bar{\bar{u}}) + \frac{1}{\cos\phi}\frac{\partial}{\partial y}(\pi v\cos\phi)$$

[AL, Eq. (166)]. The row vector $\langle \mathbf{N}_2\rangle^T$ is given in the Appendix.

The thermodynamic equation (AL, p. 209) is

$$\frac{\partial}{\partial t}(\pi T_k) + \nabla\cdot(\pi\mathbf{v}_k T_k) + \frac{1}{\Delta\sigma_k}\{(\pi\dot{\sigma})_{k+1/2}P_k\hat{\theta}_{k+1/2} - (\pi\dot{\sigma})_{k-1/2}P_k\hat{\theta}_{k-1/2}\} = \frac{1}{c_p}(\sigma\pi\alpha)_k\left(\frac{\partial}{\partial t} + \mathbf{v}_k\cdot\nabla\right)\pi + \frac{\pi}{c_p}Q_k, \tag{6}$$

where the subscripts are level indices; θ is the potential temperature; $P \equiv T/\theta \equiv (p/1000)^\kappa$; and C_p specific heat at constant pressure. Integration of the continuity equation gives $\langle \pi\dot{\sigma}\rangle = [\mathbf{N}_1]\langle \mathbf{D}\rangle$, where $[\mathbf{N}_1]$ is given in the Appendix. Thus, (6) can be written as

$$\frac{\partial}{\partial t}(\pi T_k) + \overline{\overline{T_k}}D_k + \frac{1}{c_p}(\sigma\pi\alpha)_k\langle \mathbf{N}_2\rangle^T\langle \mathbf{D}\rangle + ([\mathbf{M}_4]\langle \mathbf{D}\rangle)_k = R_{T_k},$$

or as

$$\frac{\partial}{\partial t}(\pi\langle \mathbf{T}\rangle) + [\mathbf{M}_2]\langle \mathbf{D}\rangle = \langle \mathbf{R}_T\rangle, \tag{7}$$

where $[\mathbf{M}_4]\langle \mathbf{D}\rangle$ denotes the linear portion of the terms involving $\dot{\sigma}$, and R_T denotes the heating and all nonlinear terms. The matrices $[\mathbf{M}_2]$ and $[\mathbf{M}_4]$ are given in the Appendix. Instead of π, $\bar{\bar{\pi}}$ is used in computing $[\mathbf{M}_4]$. The difference created in this procedure becomes part of R_T.

Eqs. (3), (4), (5), (6) and the hydrostatic equation form the complete set of governing equations in the model. When $R_u = R_v = R_T = 0$, these equations govern the linear gravity waves in an undisturbed atmosphere.

b. The Explicit-Multiple-Time-Step Scheme

In the UCLA model, ϕ_a is related to the temperature in a nonlinear fashion [AL, Eqs. (207), (208)]. This fact will be denoted by a subscript N, thus $(\phi_a)_N$. However, one important requirement in the EMTSS is that ϕ_a must be linearly related to temperature, to make the modal decomposition (described later) possible. This requirement is met by a previous definition of ϕ_a in the UCLA model (Arakawa, 1972; and the Appendix of this paper), and this will be denoted by a subscript L, thus $(\phi_a)_L$. Thus, the hydrostatic equation has the form: $\langle \phi_a\rangle_L = [\mathbf{M}_1]\langle \mathbf{T}\rangle$, where $[\mathbf{M}_1]$ is given in the Appendix. The matrix $[\mathbf{M}_1]$ is a function of π, when p_T in Eq. (1) is not equal to zero; therefore, it is a function of the horizontal coordinates. To make the modal decomposition possible, $[\mathbf{M}_1]$ computed with $\bar{\bar{\pi}}$ will be used for all locations. In so doing, the definition of $\langle \phi_a\rangle_L$ is modified.

Following the incorporation of the foregoing ar-

guments, (3) should be rewritten as

$$\frac{\partial}{\partial t}(\pi u) + \frac{\partial}{\partial x}\bar{\bar{\Phi}}_N = R_u . \quad (8)$$

When the standard leapfrog scheme is employed, (8) becomes

$$(\pi u)^{t-\Delta t+2\Delta\tau} - (\pi u)^{t-\Delta t} + 2\Delta\tau \frac{\partial}{\partial x}(\bar{\bar{\Phi}})_N{}^{t-\Delta t+\Delta\tau} = 2\Delta\tau R_u{}^{t-\Delta t+\Delta\tau}, \quad (9)$$

where Δt is a time interval allowed by the CFL limit, based on the speed of meteorological waves, and $\Delta\tau = \Delta t/n$, where n is the smallest integer (usually 5) such that $\Delta\tau$ is less than the CFL limit, based on the fastest gravity waves. Marching (9) with $2\Delta\tau$ intervals between $t - \Delta t$ and $t + \Delta t$ and summing up the results gives

$$(\pi u)^{t+\Delta t} - (\pi u)^{t-\Delta t} + 2\Delta t \frac{\partial}{\partial x}(\bar{\tilde{\Phi}})_N{}^{2\Delta t} = 2\Delta t \tilde{R}_u{}^{2\Delta t} \approx 2\Delta t R_u{}^t, \quad (10)$$

where $(\tilde{\ })^{2\Delta t}$ is the arithmetic averaging over the $2\Delta t$ interval. With regard to the stability of the scheme, the approximation of $\tilde{R}_u{}^{2\Delta t}$ by $R_u{}^t$ is allowed, since R_u does not create a high frequency variation in πu. This approximation introduces a truncation error which, however, does not create linear instability. When the term

$$2\Delta t \frac{\partial}{\partial x}(\bar{\bar{\tilde{\Phi}}}_L{}^{2\Delta t} - \bar{\bar{\tilde{\Phi}}}_N{}^{2\Delta t} - \bar{\bar{\Phi}}_L{}^t)$$

is added to both sides, (10) becomes

$$\begin{aligned}(\pi u)^{t+\Delta t} - (\pi u)^{t-\Delta t} &+ 2\Delta t \frac{\partial}{\partial x}(\bar{\bar{\tilde{\Phi}}}_L{}^{2\Delta t} - \bar{\bar{\Phi}}_L{}^t) \\ &= 2\Delta t R_u{}^t + 2\Delta t \frac{\partial}{\partial x}(\bar{\bar{\tilde{\Phi}}}_L{}^{2\Delta t} - \bar{\bar{\tilde{\Phi}}}_N{}^{2\Delta t} - \bar{\bar{\Phi}}_L{}^t) \\ &\approx 2\Delta t R_u{}^t + 2\Delta t \frac{\partial}{\partial x}(\bar{\bar{\Phi}}_L{}^t - \bar{\bar{\Phi}}_N{}^t - \bar{\bar{\Phi}}_L{}^t) \\ &= 2\Delta t R_u{}^t - 2\Delta t \frac{\partial}{\partial x}\bar{\bar{\Phi}}_N{}^t. \quad (11)\end{aligned}$$

The right side of (11) gives the change of πu over the $2\Delta t$ interval in one leapfrog step. Therefore, (11) becomes

$$(\pi u)^{t+\Delta t} - (\pi u)^{t-\Delta t} + 2\Delta t \frac{\partial}{\partial x}(\bar{\bar{\tilde{\Phi}}}_L{}^{2\Delta t} - \bar{\bar{\Phi}}_L{}^t) = (\pi u)_E{}^{t+\Delta t} - (\pi u)^{t-\Delta t}, \quad (12)$$

where the subscript E denotes the results from marching once with the $2\Delta t$ interval without the help of the EMTSS scheme. Thus, $(\pi u)^{t+\Delta t}$ can be found by marching (8) over $2\Delta t$ with time step Δt only once, if $\tilde{\Phi}_L{}^{2\Delta t}$ is known.

Similarly, the other prognostic equations are

$$(\pi v)^{t+\Delta t} - (\pi v)^{t-\Delta t} + 2\Delta t \frac{\partial}{\partial y}(\tilde{\Phi}_L{}^{2\Delta t} - \Phi_L{}^t) = (\pi v)_E{}^{t+\Delta t} - (\pi v)^{t-\Delta t}, \quad (13)$$

$$\langle \pi \mathbf{T} \rangle^{t+\Delta t} - \langle \pi \mathbf{T} \rangle^{t-\Delta t} + 2\Delta t [\mathbf{M}_2] \langle \tilde{\mathbf{D}}^{2\Delta t} - \mathbf{D}^t \rangle = \langle \pi \mathbf{T} \rangle_E{}^{t+\Delta t} - \langle \pi \mathbf{T} \rangle^{t-\Delta t}, \quad (14)$$

$$\pi^{t+\Delta t} - \pi^{t-\Delta t} + 2\Delta t \langle \mathbf{N}_2 \rangle^T \langle \tilde{\mathbf{D}}^{2\Delta t} - \mathbf{D}^t \rangle = \pi_E{}^{t+\Delta t} - \pi^{t-\Delta t}. \quad (15)$$

Since the aim now is to obtain the two sets of unknowns, $\langle \tilde{\Phi} \rangle^{2\Delta t}$ and $\langle \tilde{\mathbf{D}} \rangle^{2\Delta t}$, the four sets of equations can be reduced to two sets. Forming $[\mathbf{M}_1]$ (14) + $\langle \sigma\pi\alpha - \phi_L \rangle$ (15) gives

$$\langle \Phi_L \rangle^{t+\Delta t} - \langle \Phi_L \rangle^{t-\Delta t} + 2\Delta t [\mathbf{M}_3] \langle \tilde{\mathbf{D}}^{2\Delta t} - \mathbf{D}^t \rangle = \langle \Phi_L \rangle_E{}^{t+\Delta t} - \langle \Phi_L \rangle^{t-\Delta t}, \quad (16)$$

where $[\mathbf{M}_3] \equiv [\mathbf{M}_1][\mathbf{M}_2] + \overline{\overline{\langle \sigma\pi\alpha - \phi_L \rangle}} \langle \mathbf{N}_2 \rangle^T$. The grid scheme C (AL, p. 182) used in the UCLA model is not changed.

In order to form the divergence equation from (12) and (13), it is convenient to define π at the $u(v)$ points as the average of the two neighboring π's in the zonal (meridional) direction. However, it should be emphasized that the original definition of π at the u and v points (AL, p. 242) are still used in computing $u_E{}^{t+\Delta t}$ and $v_E{}^{t+\Delta t}$.

Eqs. (12) and (13) give the divergence equation

$$\langle \mathbf{D} \rangle^{t+\Delta t} - \langle \mathbf{D} \rangle^{t-\Delta t} + 2\Delta t \nabla^2 \langle \tilde{\Phi}_L{}^{2\Delta t} - \Phi_L{}^t \rangle = \langle \mathbf{D} \rangle_E{}^{t+\Delta t} - \langle \mathbf{D} \rangle^{t-\Delta t}, \quad (17)$$

where

$$\nabla^2 = \frac{\bar{\bar{\partial^2}}}{\partial x^2} + \frac{1}{\cos\phi}\frac{\partial}{\partial y}\left(\cos\phi \frac{\partial}{\partial y}\right).$$

Note that the dashed overbar operator is used twice. The basic EMTSS is to use (16) and (17) in the $\Delta\tau$ interval, where they are written as

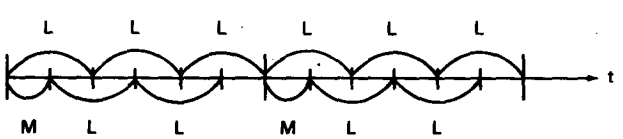

FIG. 1. Schematic representation of the time differencing scheme of the model showing a sequence of usage of leapfrog schemes (L) and the Matsuno schemes (M). Small time steps are not shown because they are different for different modes.

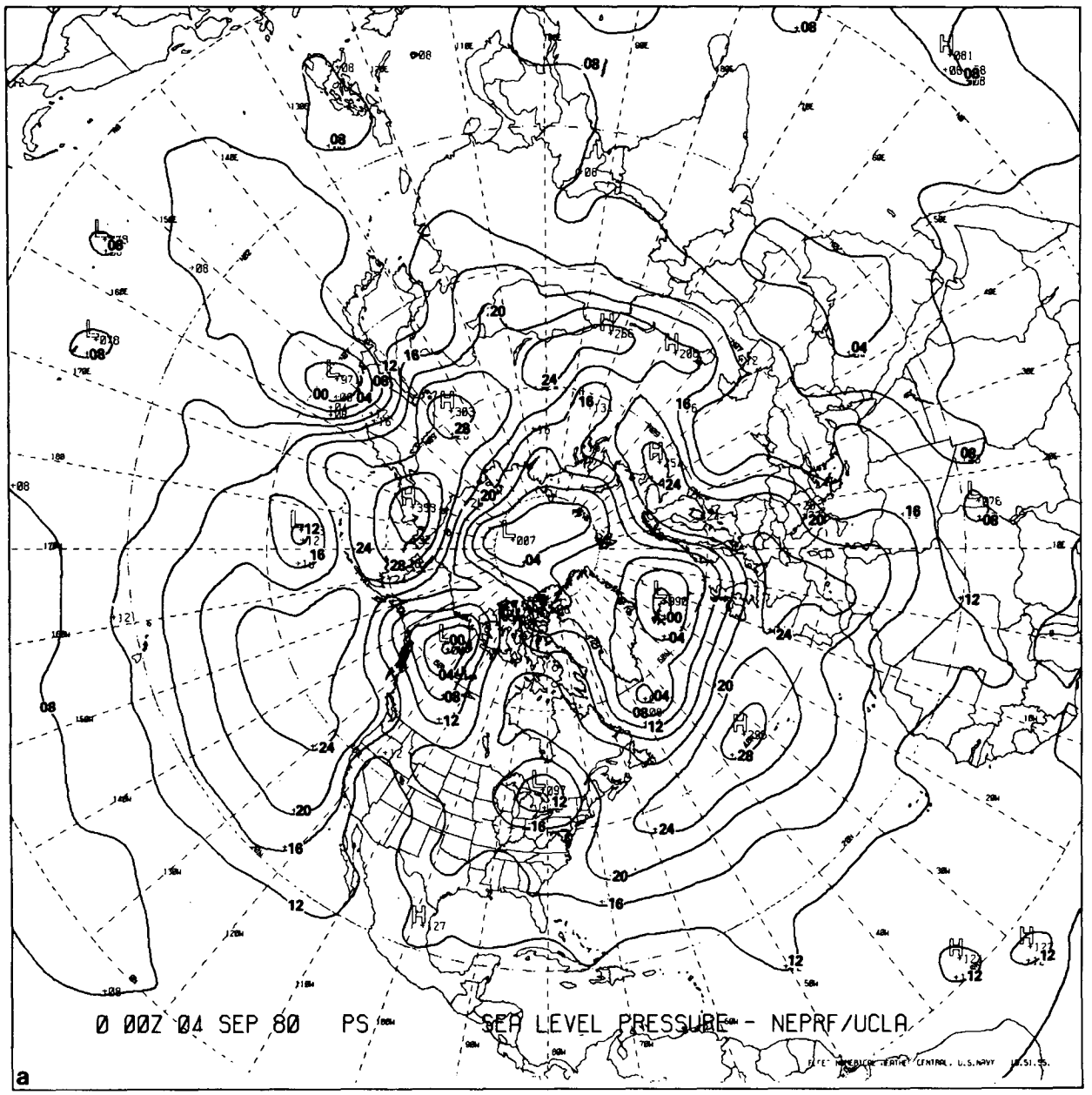

FIG. 2a. Initial sea level pressure (mb), Northern Hemisphere.

$$\langle \Phi_L \rangle^{\tau+\Delta\tau} - \langle \Phi_L \rangle^{\tau-\Delta\tau} + 2\Delta\tau[\mathbf{M}_3]\langle \mathbf{D}^{\tau} - \mathbf{D}^{t} \rangle = \left(\frac{\Delta\tau}{\Delta t}\right)(\langle \Phi_L \rangle_E^{t+\Delta t} - \langle \Phi_L \rangle^{t-\Delta t}), \quad (18)$$

$$\langle \mathbf{D} \rangle^{\tau+\Delta\tau} - \langle \mathbf{D} \rangle^{\tau-\Delta\tau} + 2\Delta\tau\nabla^2\langle \Phi_L{}^{\tau} - \Phi_L{}^{t} \rangle = \left(\frac{\Delta\tau}{\Delta t}\right)(\langle \mathbf{D} \rangle_E^{t+\Delta t} - \langle \mathbf{D} \rangle^{t-\Delta t}), \quad (19)$$

and to march these two equations with fixed right sides with time step $\Delta\tau$ between $t - \Delta t$ and $t + \Delta t$ (a Matsuno scheme has to be used in the first marching step). The two unknowns, $\langle \tilde{\Phi} \rangle^{2\Delta t}$ and $\langle \tilde{\mathbf{D}} \rangle^{2\Delta t}$, can be obtained by taking arithmetic average of the results of the marching.

Thus far, the number of equations that are required to be marched with a $\Delta\tau$ time step has been reduced from $3K + 1$ to $2K$, where K is the number of vertical levels in the model. A further reduction can be achieved by adopting a modal decomposition method (Burridge, 1975). Eqs. (18) and (19) can be decomposed into independent modes by multiplication with the inverse of the matrix $[\mathbf{E}]$, whose columns are the eigenvectors of $[\mathbf{M}_3]$. The results of the multiplication,

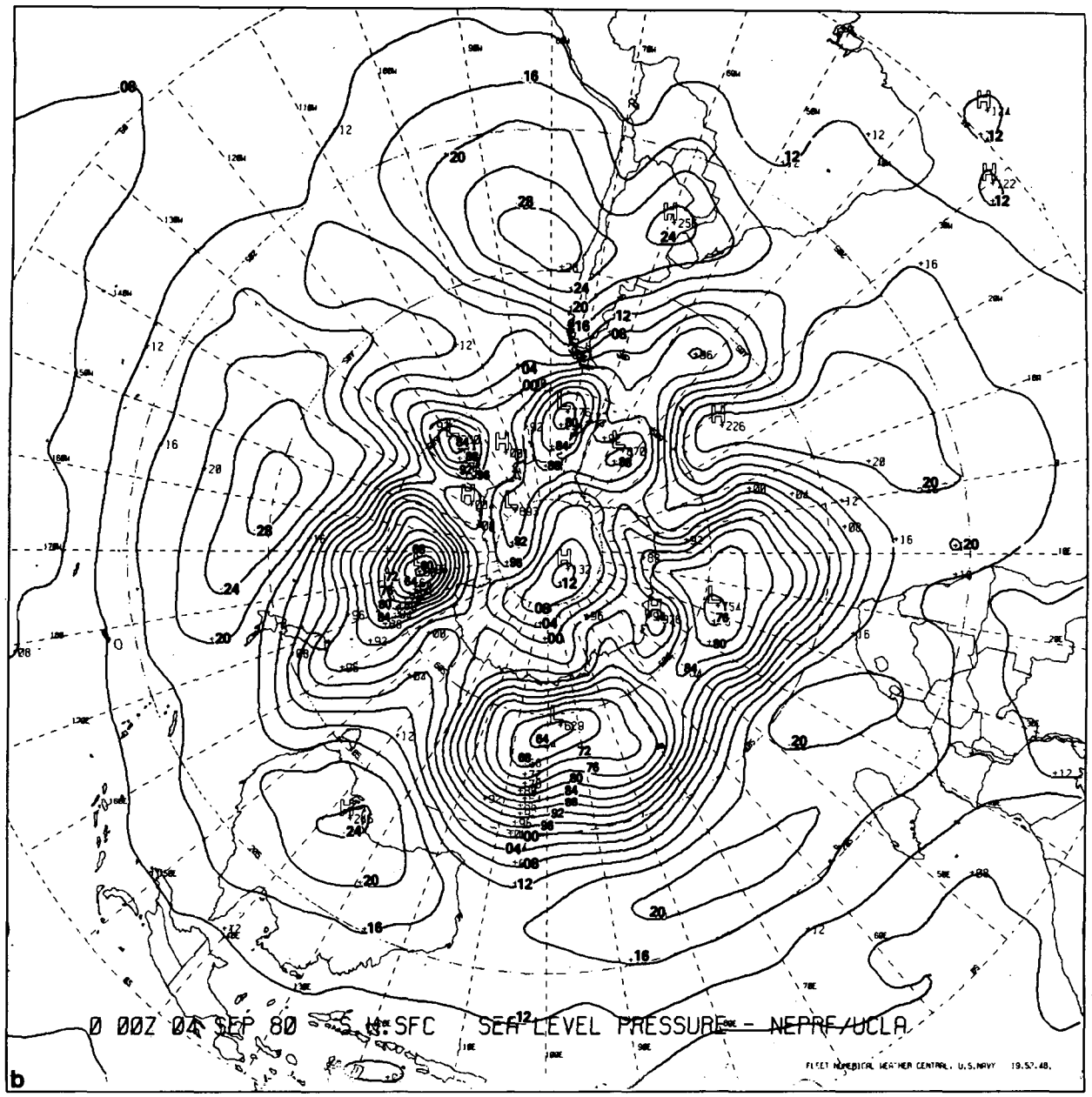

FIG. 2b. As in (a), but for the Southern Hemisphere.

which govern the different gravity modes, are

$$(\langle \Phi_L{}^E \rangle^{\tau+\Delta\tau} - \langle \Phi_L{}^E \rangle^t) - (\langle \Phi_L{}^E \rangle^{\tau-\Delta\tau} - \langle \Phi_L{}^E \rangle^t) + 2\Delta\tau[\lambda]\langle \mathbf{D}^{E\tau} - \mathbf{D}^{Et} \rangle = \left(\frac{\Delta\tau}{\Delta t}\right)[\mathbf{E}]^{-1}(\langle \Phi_L \rangle_E{}^{t+\Delta t} - \langle \Phi_L \rangle^{t-\Delta t}), \quad (20)$$

$$(\langle \mathbf{D}^E \rangle^{\tau+\Delta\tau} - \langle \mathbf{D}^E \rangle^t) - (\langle \mathbf{D}^E \rangle^{\tau-\Delta\tau} - \langle \mathbf{D}^E \rangle^t) + 2\Delta\tau\nabla^2\langle \Phi_L{}^{E\tau} - \Phi_L{}^{Et} \rangle = \left(\frac{\Delta\tau}{\Delta t}\right)[\mathbf{E}]^{-1}(\langle \mathbf{D} \rangle_E{}^{t+\Delta t} - \langle \mathbf{D} \rangle^{t-\Delta t}), \quad (21)$$

where $[\lambda]$ is equal to $[\mathbf{E}]^{-1}[\mathbf{M}_3][\mathbf{E}]$, a diagonal matrix whose diagonal elements are the eigenvalues of $[\mathbf{M}_3]$ (i.e., the square of the phase speeds of the gravity wave modes in an undisturbed atmosphere), and $\langle \mathbf{x} \rangle^E \equiv [\mathbf{E}]^{-1}\langle \mathbf{x} \rangle$.

Eqs. (20) and (21) are marched in the $2\Delta t$ interval with different $\Delta\tau$ for each mode, as determined by the CFL condition based on the phase speed of that mode. The right sides of (20) and (21) are, of course, held constant in this marching. The quantities $(\tilde{D}^{E2\Delta t} - D^{Et})$ and $(\tilde{\Phi}_L{}^{E2\Delta t} - \Phi_L{}^{Et})$ are obtained from arithmetically averaging the results of this marching. Only modes with phase speeds greater than the max-

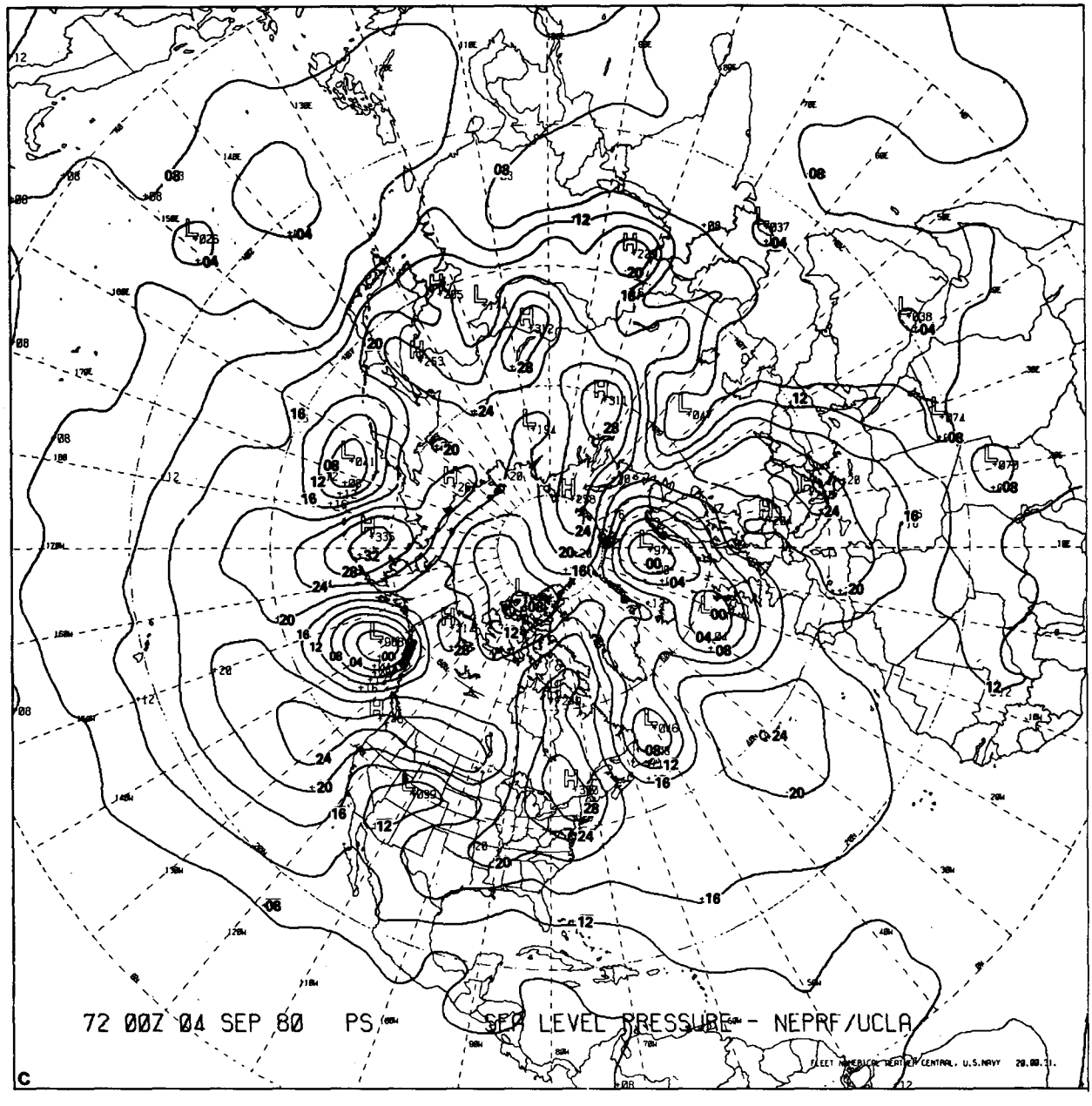

FIG. 2c. 72 h sea level pressure (mb), Northern Hemisphere, no EMTSS.

imum speed of the meteorological waves have to be marched in this manner. Other modes assume zero values for $(\tilde{D}^{E2\Delta t} - D^{Et})$ and $(\tilde{\Phi}_L{}^{E2\Delta t} - \Phi_L{}^{Et})$. Finally **[E]** is multiplied with $(\tilde{D}^{E2\Delta t} - D^{Et})$ and $(\tilde{\Phi}_L{}^{E2\Delta t} - \Phi_L{}^{Et})$ to obtain $(\tilde{D}^{2\Delta t} - D^{t})$ and $(\tilde{\Phi}_L{}^{2\Delta t} - \Phi_L{}^{t})$, respectively.

In summary, the procedure of the EMTSS method is as follows:

1) Calculate the matrices, and the eigenvalues and eigenvectors of $[\mathbf{M}_3]$, using the predetermined global mean quantities. This step is done only once.

2) Compute $(\langle\Phi_L{}^E\rangle^{t-\Delta t} - \langle\Phi_L{}^E\rangle^t$ and $\langle\mathbf{D}^E\rangle^{t-\Delta t} - \langle\mathbf{D}^E\rangle^t)$.

3) Use the larger time interval Δt, march forward one step and compute the right-hand sides of (20) and (21).

4) March (20) and (21) with different $\Delta\tau$, for different modes. For the six-level UCLA model (AL, p. 176), only the first three modes need to be integrated with $\Delta\tau = (1/5, 1/3, 1/2)\Delta t$.

5) Average the result from step (4) to obtain $(\langle\tilde{\Phi}_L\rangle^{2\Delta t} - \langle\Phi_L\rangle^t)$ and $(\langle\tilde{\mathbf{D}}\rangle^{2\Delta t} - \langle\mathbf{D}\rangle^t)$ which then allows the calculation of the predicted quantities at $t + \Delta t$ in (12) through (15).

Although the above descriptions are based on the leapfrog scheme, the changes are minor when using

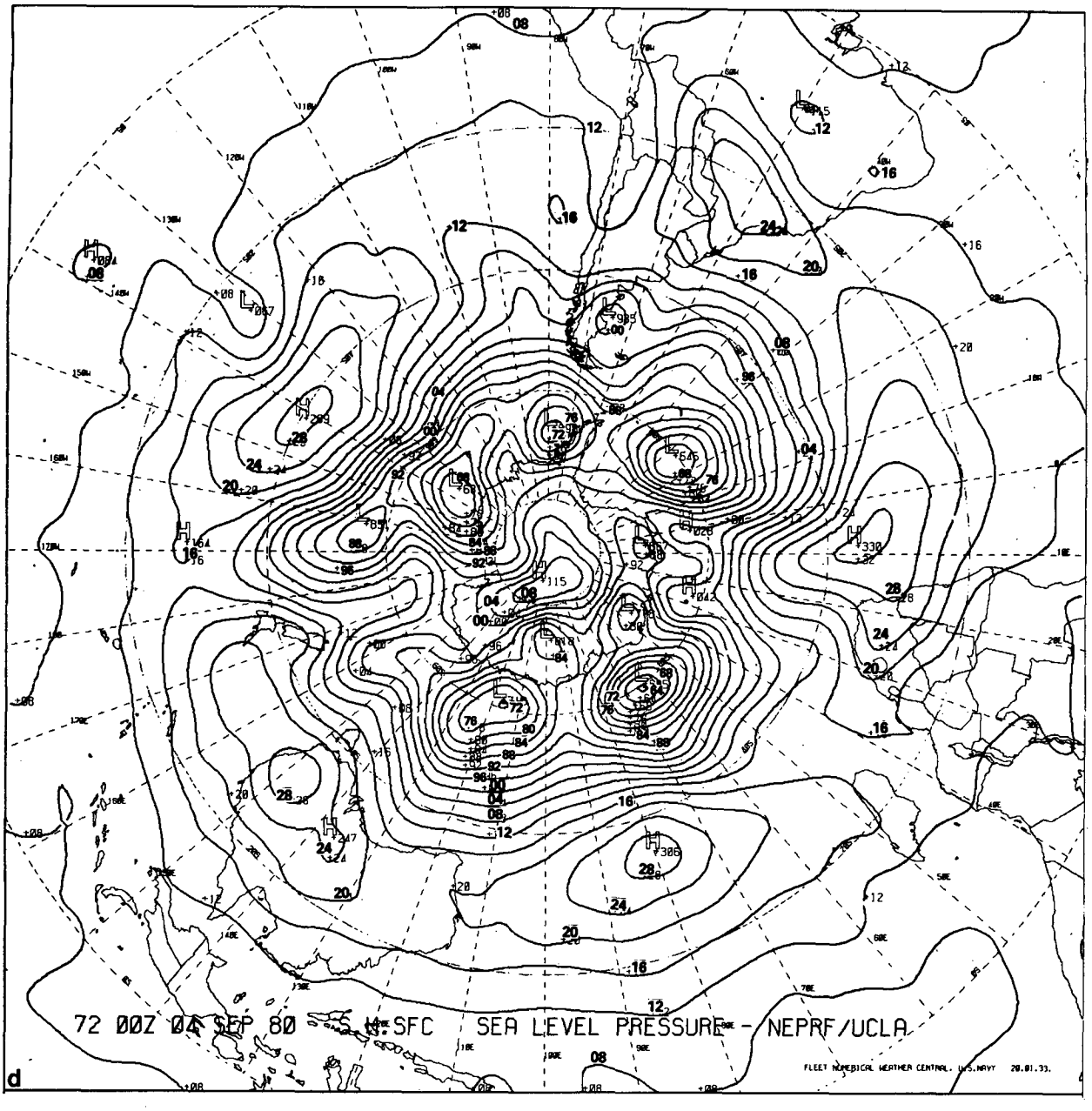

FIG. 2d. As in (c) but for the Southern Hemisphere, no EMTSS.

the Matsuno scheme, which is periodically used in the UCLA model to overcome the time splitting problem associated with the leapfrog scheme (AL, p. 260). In the first part of the Matsuno scheme, the superscripts $t + \Delta t$, $t - \Delta t$ and $2\Delta t$ in the above equations are changed to t^*, t and Δt, respectively. Then, in the second part of the Matsuno scheme, the superscripts $t - \Delta t$ and $2\Delta t$ are changed to t^* and Δt, respectively. In both parts, of course, the factor $2\Delta t$ is changed to Δt.

c. *Modification of the advective terms near the poles*

Even when Δt is increased by a factor of five, the dashed overbar operator, described in Subsection 3a, is sufficient to circumvent the problem of linear instability related to the gravity wave terms, due to the diminishing zonal grid spacing toward the poles. However, the advective terms $\partial/\partial x[(\pi u)q]$ where q denotes u, v and T, can create linear instability near the poles when Δt is enlarged. The time increment allowed for the advective terms Δt, is limited by Δt

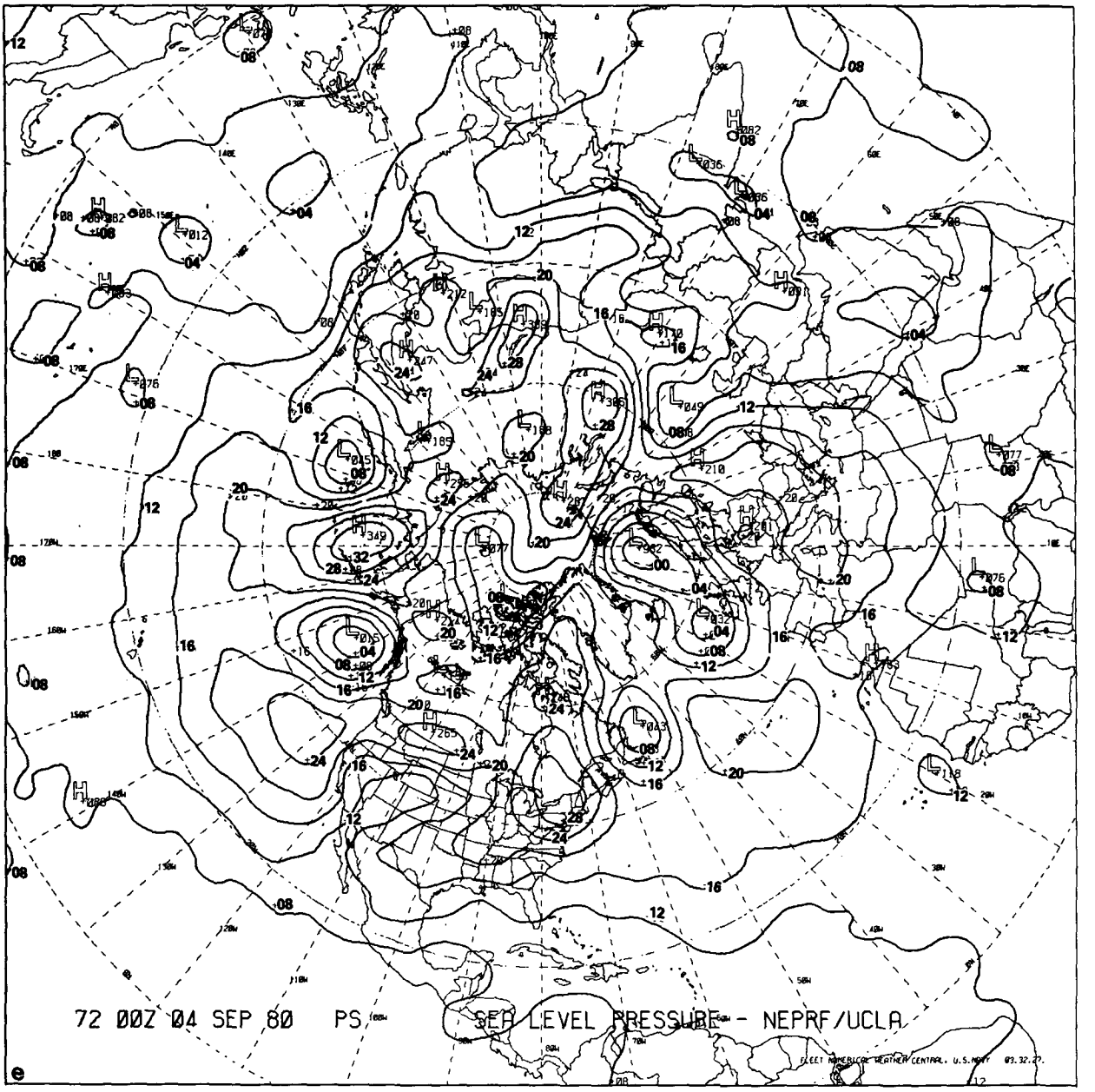

FIG. 2e. 72 h sea level pressure (mb), Northern Hemisphere, with EMTSS.

$< \epsilon\Delta x/(u + c_m)$, where c_m is the speed of the meteorological waves, u is that of the basic flow, and ϵ has a magnitude of order 1, with its exact value depending on the time differencing scheme used. When u is large in the polar region where Δx is small, Δt cannot be increased by a factor of five. The solution used here is to apply the dashed overbar operator to q in the terms $\partial/\partial x[(\pi u)q]$ in (272) and (299) of AL. Thus, in step 2 of the EMTSS procedure (Subsection 3b) the second term in (299) is changed to

$$\delta_\xi[F(\overline{\overline{T}})^\xi].$$

Here the notations follow those of AL, ξ is the curvilinear coordinate in zonal direction [(252) of AL], δ and overbar are defined in (63) and (64) of AL. Also, the changes in (272) are to substitute (275) into (272) and then apply the dashed overbar operator on u in those terms containing $\overline{F}^*$. Similar changes are made for the v component equation. Short-term tests (72 h) show this method is successful in controlling

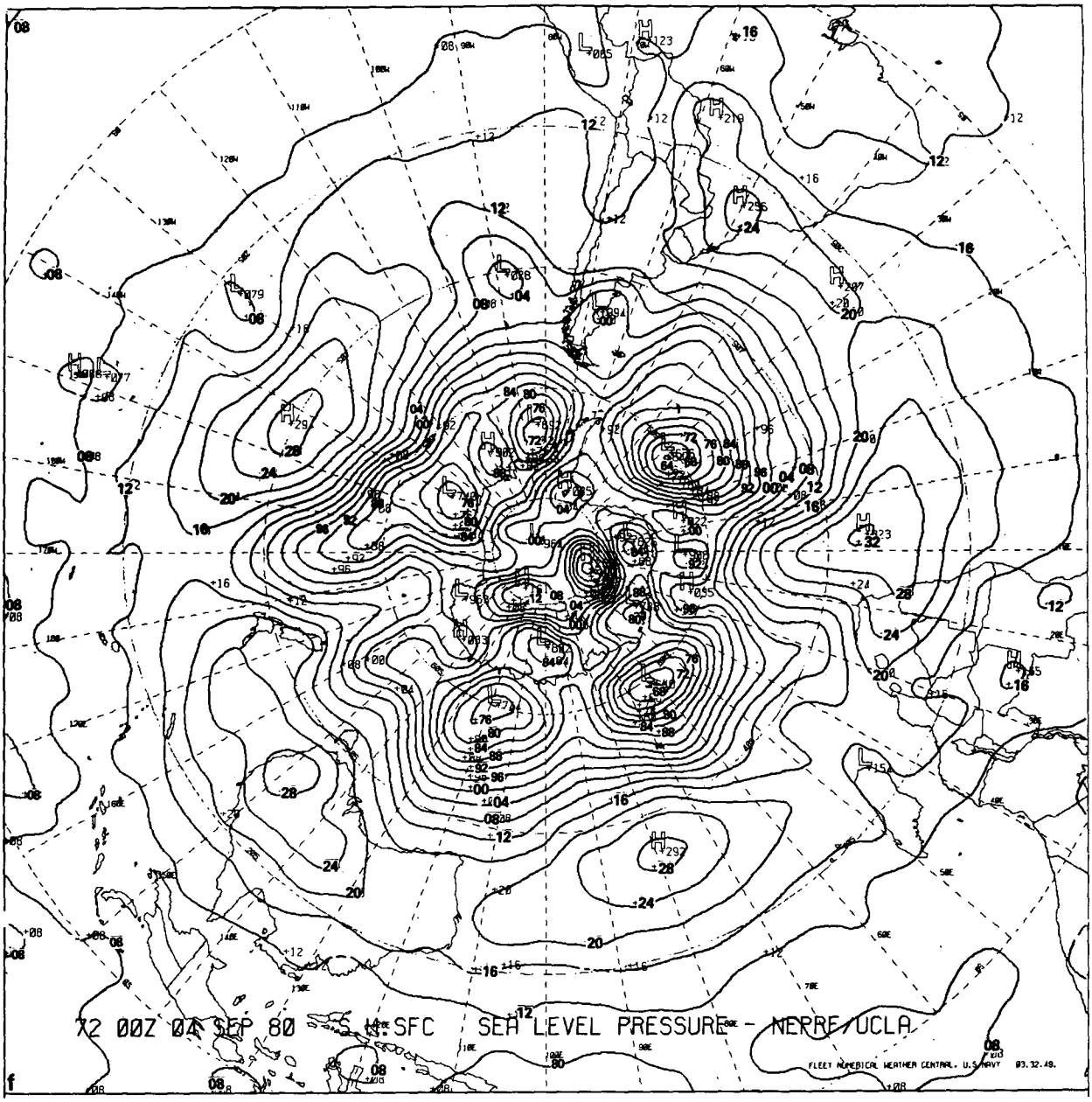

FIG. 2f. As in (e), but for Southern Hemisphere, with EMTSS.

linear instability. However, since the quadratic conservation properties no longer hold (they tend to increase square vorticity and to decrease kinetic energy) there can be some side effects in this approach, as will be shown in the result section.

d. The time differencing method

As shown in Fig. 1, the time differencing method used to calculate the dynamic terms consists of a series of the leapfrog schemes with a periodic insertion of the Matsuno scheme. The time step is Δt. The source and sink terms, and the vertical flux convergence term of the moisture equation, are calculated as an instantaneous adjustment. For $\Delta t = 30$ min, these calculations are done after each leapfrog or Matsuno step. Thus, the frequency of computing the physical processes is not changed.

e. Addition of the pressure averaging method

When the pressure averaging method (Shuman, 1971; Schoenstadt and Williams, 1976; Brown and Campana, 1978) is used, (20) and (21) can be inte-

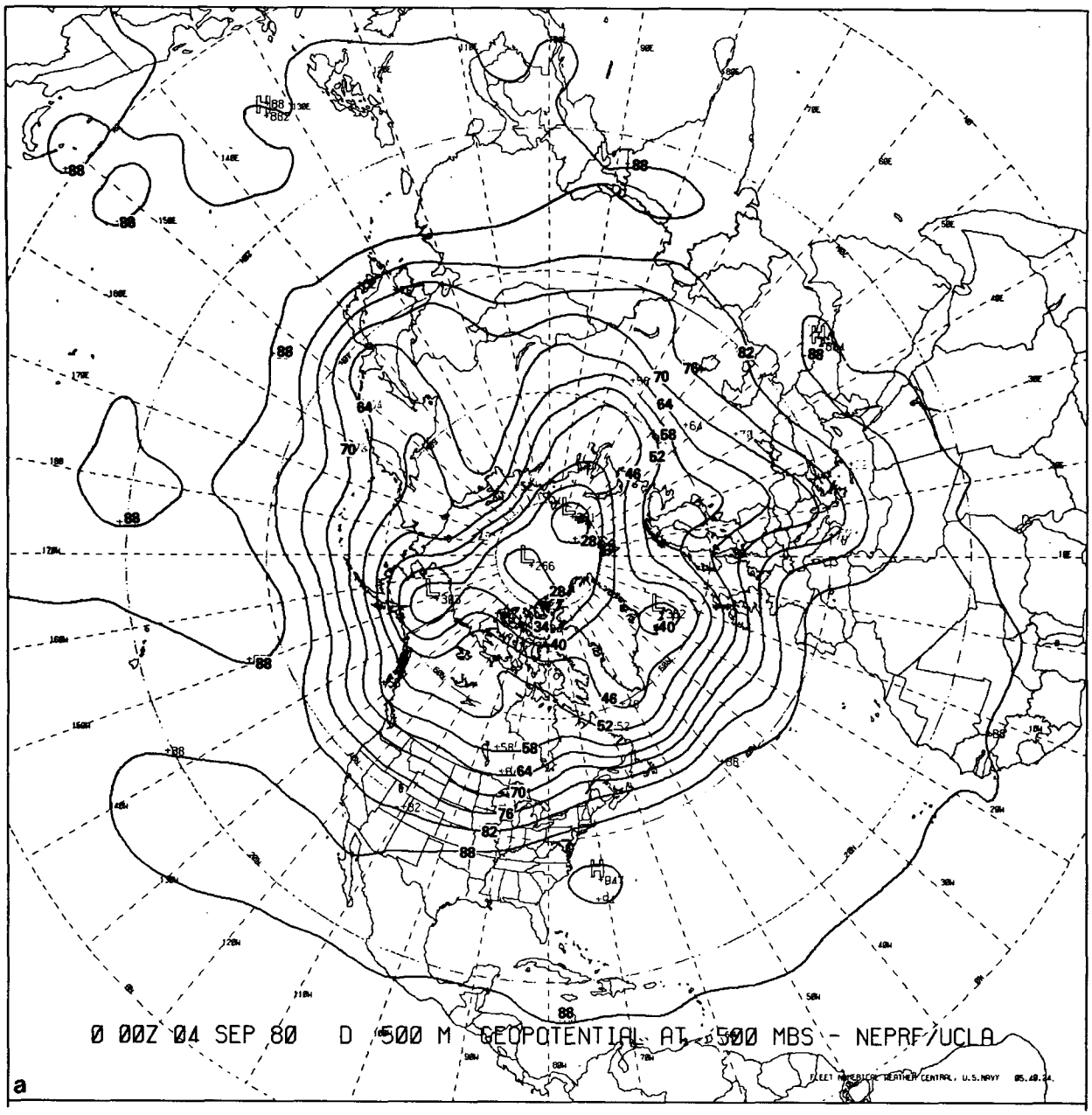

FIG. 3a. Initial 500 mb geopotential (60 m interval), Northern Hemisphere.

grated with $\Delta\tau = (1/3, 1/2, 1/1.5)\Delta t$. The value of the α parameter used here is 0.24. This method further enhances the efficiency of the EMTSS.

4. Results and discussion

The performance of the present EMTSS formulation is, of course, judged by its stability, efficiency and accuracy. The following discussions are directed toward these characteristics.

a. Stability

Two 12-h runs and one 72-h run, starting from different initial conditions, showed that the EMTSS formulation is linearly stable. Since the linear stability criterion depends not only on the wave speeds but also on the wind speed, the present formulation is best tested with a large wind speed, especially in the polar region, where the zonal grid size is small. In one 12-h test run, the wind speed near the north pole

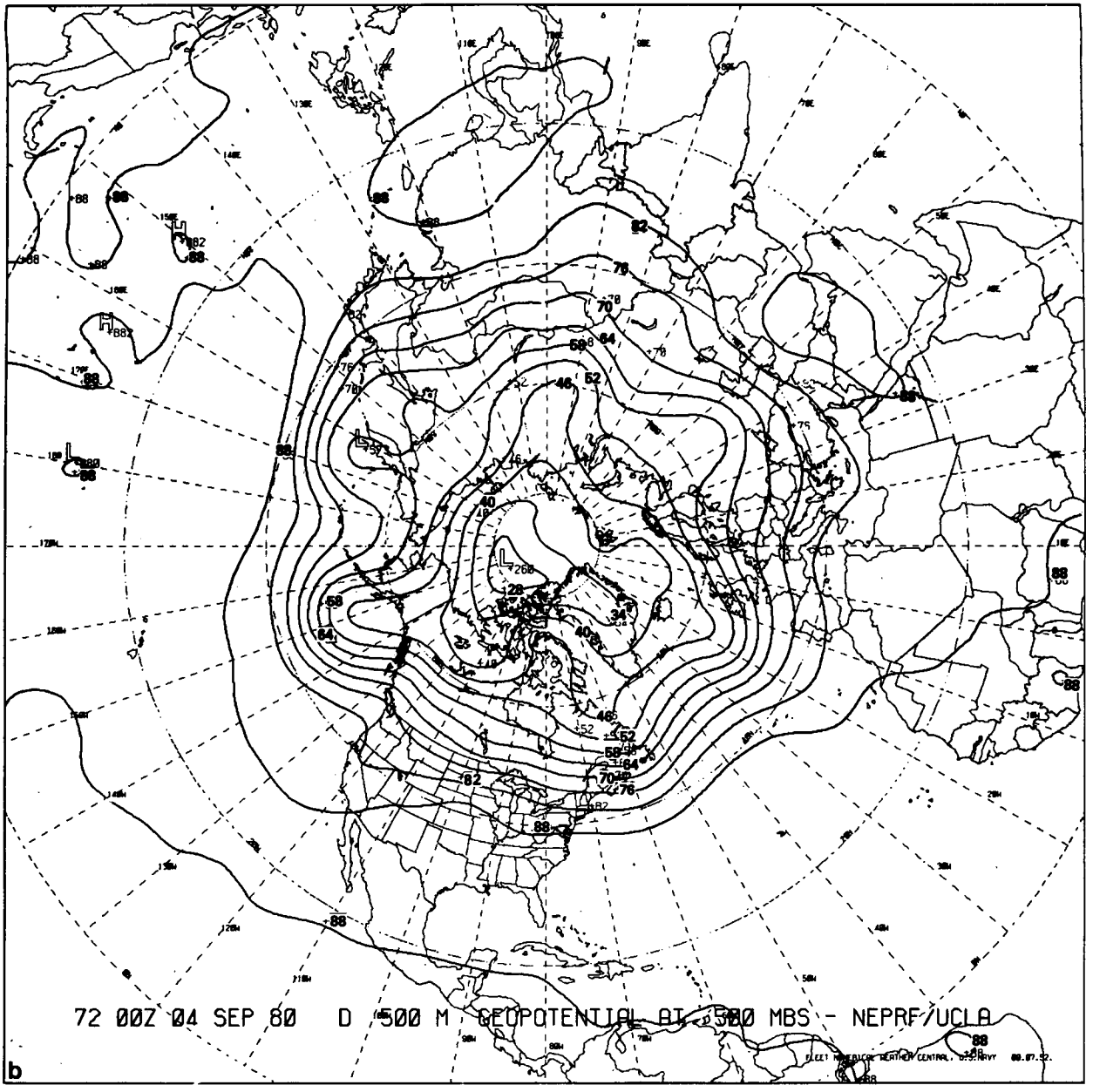

FIG. 3b. 72 h 500 mb geopotential (60 m interval), Northern Hemisphere, no EMTSS.

reached more than 50 m s^{-1} and no linear instability occurred.

b. Efficiency

Tests show that when the UCLA model with six vertical levels, $\Delta\phi = 4^0$, $\Delta\lambda = 5^0$ and $\Delta t = 30$ min (five times the original Δt) was run on a CDC 175 without physical processes, the reduction in integration CPU time by the EMTSS was 48%, of which 4% was due to the addition of the pressure averaging methods. The efficiency increases with greater vertical resolution. When vertical resolution is doubled, the time needed for ordinary explicit methods will be doubled. However, the overhead for using EMTSS only increases by a small fraction, since the number of gravity wave modes integrated with small time steps remains the same. The net reduction in CPU time for the full model depends on the amount of the CPU time used for the physical processes, which of course get no help from the EMTSS. The reduction is 24% for the full UCLA model with the previously

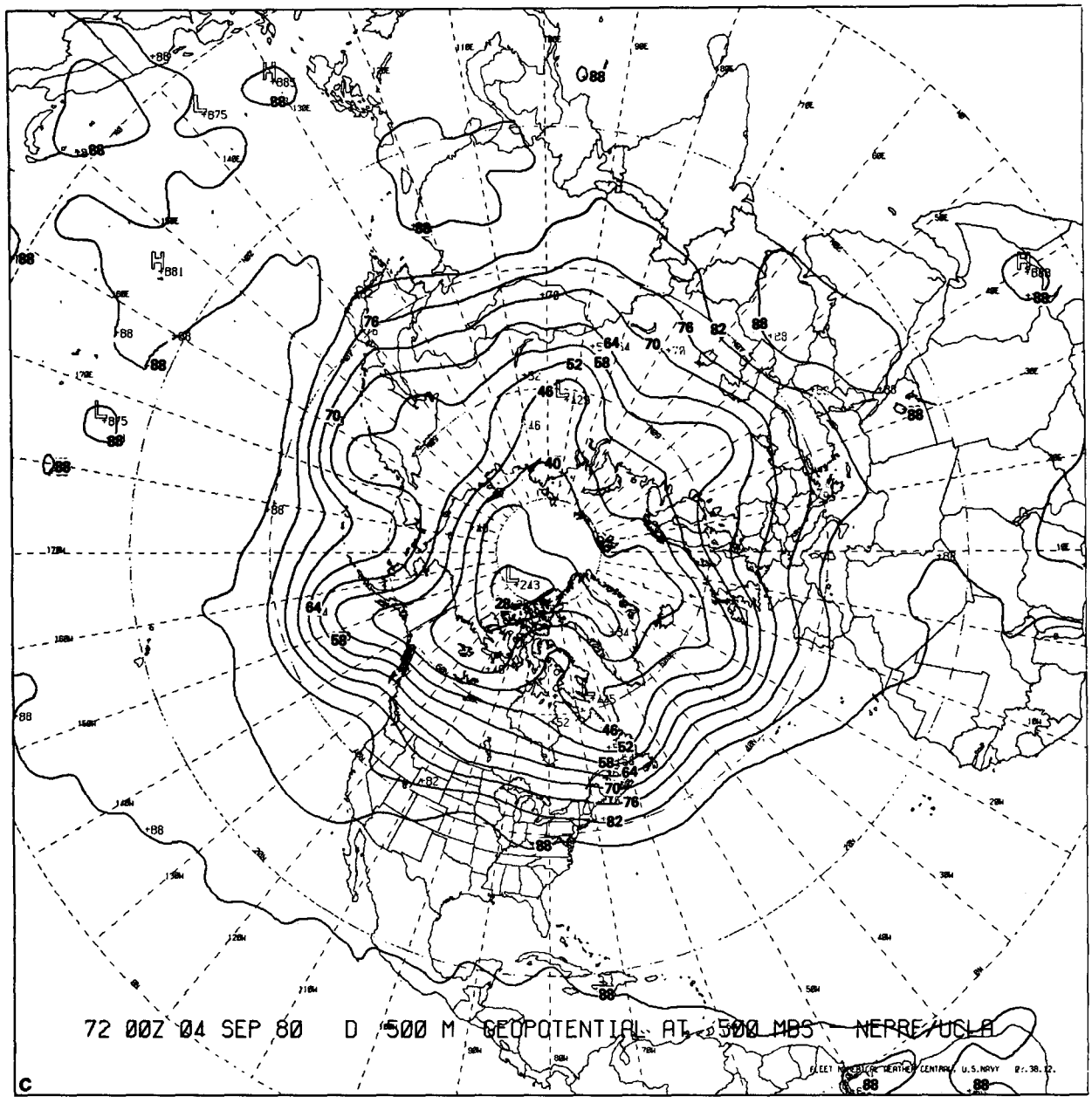

FIG. 3c. 72 h 500 mb geopotential (60 m interval), Northern Hemisphere, with EMTSS.

mentioned grid size. Only when a large portion of CPU time is used for dynamical processes does it pay to adopt the EMTSS. This occurs when horizontal resolution is increased by a large degree.

c. *Accuracy*

Two 72-h runs with and without the EMTSS were made, starting from the same well-balanced (in the sense that no large gravity wave components exist) initial conditions, which is the end of another 72-h run. The initial conditions and the results at hour 72 are shown in Figs. 2 and 3 for sea level pressure and 500 mb geopotential height, respectively. The difference between the two runs is very small, when it is compared with the changes over 72 hours. The rms difference (Table 1) in 500 mb geopotential height at hour 72 is 16 m, which is very small compared with the typical forecast error of 75 m. Also, the rms difference in 500 mb zonal wind at hour 72 is 2.4 m s^{-1} compared with the typical 48 h forecast error of 8.5 m s^{-1} (Somerville *et al.*, 1974). Although there was

TABLE 1. The rms differences.

	rms differences		
	Surface pressure (mb)	500 mb Geopotential height (m)	500 mb Zonal wind (m s^{-1})
24 h	1.09	8.93	1.03
48 h	1.54	12.40	1.79
72 h	1.97	15.78	2.40

concern whether computing the matrices using a globally averaged π was appropriate for high terrain areas, no adverse effect over these regions was detected. One obvious discrepancy between the two runs is that at hour 72, a strong high centered at (35°E, 80°S) appeared in the run using the EMTSS, whereas only a weak high occupied this region in the run without EMTSS. A separate 72 h run using the EMTSS starting from the same initial conditions but without the physical processes, also has this intense high. Thus, it is reasonable to consider this discrepancy a side effect of the modification described in Subsection 3c.

Overall, the results are remarkably good outside regions very close to the poles. The poor performance near the poles, however, is not a direct consequence of applying the EMTSS, but is related to the horizontal differencing scheme, and to the diminishing zonal grid size near the poles. Whether this problem precludes long-term integration was not answered in this study, due to the limitations on computing resources.

Acknowledgments. This work was supported by the Naval Research Laboratory under contract numbers N00173-80-C-0101 and N00014-81-C-2085. Thanks are due to Dr. Rangarao V. Madala who suggested this research. Dr. Thomas E. Rosmond of the Naval Environmental Prediction Research Facility provided the initial conditions for the test runs. His help in making the computing facility at Naval Fleet Numerical Prediction Central accessible is greatly appreciated. Thanks are also extended to Drs. Simon W. Chang, Kay E. Cheney and Darrell Strobel for reading the manuscript.

APPENDIX

Computation of the Matrices

In a K-level σ coordinate model, where $\sigma = (p - p_T)/(p_S - p_T)$, the row vector $\langle \mathbf{N}_2 \rangle^T$ is

$$\langle \mathbf{N}_2 \rangle^T = (\Delta\sigma_1, \Delta\sigma_2, \ldots, \Delta\sigma_K).$$

The hydrostatic equation for ϕ_a (Arakawa, 1972, p. 25) is

$$(\phi_a)_k - (\phi_a)_{k+1} = \frac{c_P}{2}[(\bar{p}_{k+1})^\kappa - (\bar{p}_k)^\kappa] \times \left(\frac{T_k}{\bar{p}_k{}^\kappa} + \frac{T_{k+1}}{\bar{p}_{k+1}{}^\kappa}\right), \quad [A1]$$

where $\kappa = R/c_p$, and

$$(\phi_a)_K = \sum_{k=1}^{K}\left[\bar{\pi}\sigma_k \frac{R}{\bar{p}_k}\Delta\sigma_k - (\sigma_{k+1}\beta_k + \sigma_{k-1}\alpha_k)\right]T_k, \quad (A2)$$

$$\beta_k = \begin{cases} \tfrac{1}{2}[(\bar{p}_{k+1}/\bar{p}_k)^\kappa - 1] & \text{for } k \leqslant K-1 \\ 0 & \text{for } k = K, \end{cases}$$

and

$$\alpha_k = \begin{cases} 0 & \text{for } k = 1 \\ \tfrac{1}{2}[1 - (\bar{p}_{k-1}/\bar{p}_k)^\kappa] & \text{for } k \geqslant 2. \end{cases}$$

The matrix $\mathbf{M}_1$ can be constructed from the preceding equations, where (A1) and (A2) give ϕ_k ($k = 1, \cdots K$) as a linear function of T_k ($k = 1, \cdots K$). The element $(\mathbf{M}_1)_{i,j}$ equals the ϕ_i, computed using $T_j = 1$ and $T_k = 0$ for all $k \neq j$.

$$[\mathbf{N}_1] = -\begin{pmatrix} \Delta\sigma_1 & 0\text{-------}0 \\ \Delta\sigma_1 & \Delta\sigma_2\text{-------}0 \\ & \text{----------} \\ & \text{----------} \\ \Delta\sigma_1 & \Delta\sigma_2\text{----}\Delta\sigma_K \end{pmatrix} + \begin{pmatrix} \sigma_2{}^E\Delta\sigma_1 & \sigma_2{}^E\Delta\sigma_1\text{--------}\sigma_2{}^E\Delta\sigma_K \\ \sigma_3{}^E\Delta\sigma_1 & \sigma_3{}^E\Delta\sigma_2\text{--------}\sigma_3{}^E\Delta\sigma_K \\ & \text{----------} \\ & \text{----------} \\ \sigma_{K+1}{}^E\Delta\sigma_1 & \sigma_{K+1}{}^E\Delta\sigma_2\text{---}\sigma_{K+1}{}^E\Delta\sigma_K \end{pmatrix},$$

where σ^E denotes σ at an interface between two layers as shown in Fig. A1. When $\langle \pi\dot{\sigma} \rangle = [\mathbf{N}_1]\langle \mathbf{D} \rangle$ is substituted in the thermodynamic equation, $[\mathbf{M}_2]$ and $[\mathbf{M}_4]$ can easily be constructed.

The thermodynamic equation is

$$\frac{\partial}{\partial t}(\pi T_k) + \nabla\cdot(\pi \mathbf{v}_k T_k) + \frac{1}{\Delta\sigma_k}[(\pi\dot{\sigma})_{k+1/2}P_k\hat{\theta}_{k+1/2} - (\pi\dot{\sigma})_{k-1/2}P_k\hat{\theta}_{k-1/2}] = \pi\frac{T_k}{P_k}\frac{\partial P_k}{\partial \pi}\left(\frac{\partial}{\partial t} + \mathbf{v}_k\cdot\nabla\right)\pi + \pi Q_k/c_p,$$

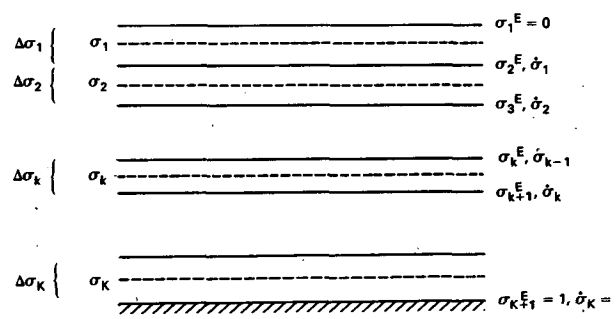

FIG. A1. Schematic diagram indicating the definitions of σ, σ^E and $\Delta\sigma$.

where

$$\pi \frac{T_k}{P_k} \frac{\partial P_k}{\partial \pi} = \frac{1}{c_p} (\sigma \pi \alpha)_k ,$$

$$\hat{\theta}_{k+1/2} = \frac{\ln \theta_k - \ln \theta_{k+1}}{(1/\theta_{k+1}) - (1/\theta_k)} .$$

Thus,

$$\frac{\partial}{\partial t} \langle \pi \mathbf{T} \rangle + [\mathbf{T}] \langle \mathbf{D} \rangle + [\mathbf{M}_4] \langle \mathbf{D} \rangle = - \left\langle \frac{\sigma \pi \alpha}{c_p} \right\rangle \langle \mathbf{N}_2 \rangle^T \langle \mathbf{D} \rangle + \langle \mathbf{R} \rangle_T ,$$

where

$$[\mathbf{T}] = \begin{pmatrix} \bar{T}_1 & 0 \text{----} 0 \\ 0 & \bar{T}_2 \text{-----} \\ \text{----------} & \\ 0 \text{-------} & \bar{T}_K \end{pmatrix} ,$$

and

$$[\mathbf{M}_4]_{k,j} = (V_{k,j} P_k \hat{\theta}_{k+1/2} - V_{k-1,j} P_k \hat{\theta}_{k-1/2}) / \Delta \sigma_k ,$$

where $V \equiv [\mathbf{N}_1]$, and

$$[\mathbf{M}_2] = [\mathbf{M}_4] + [\mathbf{T}] + \frac{1}{c_p} \begin{pmatrix} (\sigma \pi \alpha)_1 \langle \mathbf{N}_2 \rangle^T \\ \vdots \\ \vdots \end{pmatrix} .$$

It should be emphasized here that all quantities in the matrices are computed using the globally averaged temperature and surface pressure.

REFERENCES

Arakawa, A., 1972: Design of the UCLA general circulation model. Numerical simulation of weather and climate. Tech. Rep. 7, Dept. Meteor., University of California, Los Angeles, 116 pp.

——, and Lamb, V. R., 1977: Computational design of the UCLA general circulation model. *Methods in Computational Physics*, Vol. 17, Academic Press, 173–265.

Brown, J. A., and K. Campana, 1978: An economical time-differencing system for numerical weather prediction. *Mon. Wea. Rev.*, **106**, 1125–1136.

Burridge, D. M., 1975: A split semi-implicit reformulation of the Bushby–Timpson 10-level model. *Quart. J. Roy. Meteor. Soc.*, **101**, 777–792.

Courant, R., K. Friedrichs and H. Lewy, 1928: Uber die partiellen Differenzengleichungen der Mathematischen. *Phys. Math. Ann.*, **100**, 32–74.

Gadd, A. J., 1978: A split explicit integration scheme for numerical weather prediction. *Quart. J. Roy. Meteor. Soc.*, **104**, 569–582.

Kwizak, M., and A. J. Robert, 1971: A semi-implicit scheme for grid point atmospheric models of the primitive equations. *Mon. Wea. Rev.*, **99**, 32–36.

Madala, R. V., 1981: Efficient time integration schemes for atmosphere and ocean models. *Finite-difference Techniques for Vectorized Fluid Dynamics Calculations*, D. Book, Ed., *Series in Computational Physics*, Springer-Verlag, 56–74.

Marchuk, G. I., 1974: *Numerical Methods in Weather Prediction.* Academic Press, 277 pp.

Messinger, F., and A. Arakawa, 1976: Numerical methods used in atmospheric models. WMO-ICSU GARP Publ. Ser. No. 17, 64 pp.

Robert, A. J., 1969: The integration of a spectral model of the atmosphere by the implicit method. *Proc. WMO/IUGG Symp. on Numerical Weather Prediction*, Tokyo, Japan Meteor. Agency, **VII**, 19–24 pp.

Robert, A. J., J. Henderson and C. A. Turnbull, 1972: An implicit time integration scheme for baroclinic models of the atmosphere. *Mon. Wea. Rev.*, **100**, 329–335.

Schoenstadt, A. L., and R. T. Williams, 1976: The computational stability properties of the Shuman pressure gradient averaging technique. *J. Comput. Phys.*, **21**, 166–177.

Shuman, F. G., 1971: Resuscitation of an integration procedure. NMC Office Note 54, 55 pp. [NMC, National Weather Service, NOAA, Washington, DC 20233].

Somerville, R., P. H. Stone, M. Halem, J. E. Hansen, J. S. Hogan, L. M. Druyan, G. Russell, A. A. Lacis, W. J. Quirk and J. Teneneaum, 1974: GISS Model of the global atmosphere. *J. Atmos. Sci.*, **31**, 84–117.